Pharm Res (2016) 33:2517–2529
DOI 10.1007/s11095-016-1976-3

RESEARCH PAPER

Intratracheal Administration of Hyaluronan-Cisplatin Conjugate Nanoparticles Significantly Attenuates Lung Cancer Growth in Mice

Susumu Ishiguro[1] • Shuang Cai[2,3] • Deepthi Uppalapati[1] • Katie Turner[1] • Ti Zhang[2] • Wai Chee Forrest[3] • M. Laird Forrest[2,3] • Masaaki Tamura[1]

Received: 14 April 2016 / Accepted: 16 June 2016 / Published online: 22 June 2016

ABSTRACT

Purpose To determine aerosol administration capability and therapeutic efficacy of the new formulation of hyaluronan cisplatin conjugates, HylaPlat™ (HA-Pt), for lung cancer treatment.

Methods *In vitro* formulation stability test, 2D and 3D spheroid cell culture and *in vivo* efficacy studies using mouse orthotopic allograft models were conducted.

Results The HA-Pt effectively attenuated cell growth in 2D and 3D cultures with IC_{50} of 2.62 and 5.36 μM, respectively, which were comparable to those with unconjugated control cisplatin-dependent growth inhibition (IC_{50} 1.64 and 4.63 μM, respectively). A single dose of either 7.5 or 15 mg/kg HA-Pt (cisplatin equivalent) by intratracheal aerosol spray 7 days after Lewis lung carcinoma (LLC) cell inoculation markedly inhibited growth of LLC allografts in mouse lungs and resulted in a 90 or 94% reduction of tumor nodule numbers, respectively, as compared to those from the PBS control. Cancer stem cells and cisplatin resistant cells marker, CD44 expression decreased in the tumor nodules of the HA-Pt but not in those of cisplatin treated groups.

Conclusions The current study suggests that an intratracheal aerosol administration of the HA-Pt nanoparticles offers an effective strategy for lung cancer treatment and this treatment may induce only limited cisplatin resistance.

KEY WORDS apoptosis · CD44 · hyaluronan-cisplatin conjugates nanoparticle · lung cancer · pulmonary chemotherapy

ABBREVIATIONS

2D	Two dimensional
3D	Three dimensional
cfu	Colony forming units
EU	Endotoxin units
FBS	Fetal bovine serum
HA	Hyaluronan
HAdase	Hyaluronidase
HA-Pt	Hyaluronan-cisplatin nanoconjugate
IT	Intratracheal
LLC	Lewis Lung carcinoma
SEC	Size exclusion chromatography
T_g	Glass transition temperature
TUNEL	Terminal deoxynucleotidyl transferase dUTP nick end labeling
USP	US Pharmacopeia

INTRODUCTION

Lung cancer is the leading cause of cancer-related morbidity and mortality in developed countries, although its prognosis has improved due to advances in early surveillance and accurate diagnosis (1,2). However, the relative 5-year survival ratio of patients with lung cancer is still quite low (18%), with minimal improvement since the 1970's (12%). Therefore, novel treatment strategies for lung cancer are urgently needed.

Susumu Ishiguro and Shuang Cai contributed equally to this work.

Electronic supplementary material The online version of this article (doi:10.1007/s11095-016-1976-3) contains supplementary material, which is available to authorized users.

✉ Masaaki Tamura
mtamura@vet.k-state.edu

[1] Department of Anatomy & Physiology, College of Veterinary Medicine, Kansas State University, 210 Coles Hall, Manhattan, Kansas 66506, USA

[2] Department of Pharmaceutical Chemistry, School of Pharmacy, University of Kansas, Lawrence, Kansas 66047, USA

[3] HylaPharm LLC, Lawrence, Kansas 66047, USA

In order to develop successful chemotherapies, it is essential to improve anticancer efficiency and bioavailability while minimizing toxicity *in vivo*. Encapsulation of chemotherapeutics into nanoparticles has such potential, as they can be designed to increase cellular uptake in cancer tissues and to target delivery (3–6). This would reduce chemotherapeutic exposure to normal tissues, thus minimizing toxicity. However, their clinical efficacy has been limited because systemically administered nanomedicines tend to be rapidly cleared from circulation by mononuclear phagocytic cells (3). On the contrary, local administration of nanomedicines possesses a significant potential for effective clinical application. Local application allows relatively higher doses in cancer tissues, yet reduces overall doses of therapeutics (4,5).

Cisplatin is a very potent chemotherapeutic agent for multiple cancers (7–9), and has been recommended as a first line cytotoxic chemotherapeutic for multiple cancers, including non-small cell lung cancer (10,11). However, since cisplatin is known to be associated with several severe dose-limiting toxicities, several dosing strategies have been developed to reduce toxicities (11,12), including the less toxic analogue carboplatin (12) and liposomal encapsulation of cisplatin (13,14). Though cisplatin-induced renal toxicity is alleviated using an alternative carboplatin therapy in some patients, carboplatin does not demonstrate equivalent efficacy in all cisplatin sensitive tumors, and it is FDA-approved only for treatment of non-small cell lung cancer and ovarian cancers (15).

Recently, a hyaluronan-cisplatin nanoconjugate (HA-Pt) has been developed and demonstrated to be useful in preclinical studies for loco-regional therapy of multiple cancers, including head and neck squamous cell carcinoma (16–18), breast cancer (19), melanoma (20), and soft tissue sarcoma (21). Hyaluronan (HA) is an inert, naturally-occurring glycosaminoglycan polysaccharide found in the extracellular matrix of most mammalian connective tissues (22). Thus, the hyaluronan conjugate is considered to be a safe carrier for cisplatin. Furthermore, HA targets tumor cells through specific interactions of the HA polymer with the CD44 receptor (23,24), which is highly overexpressed in many cancers, including lung cancer (25,26). While CD44 is expressed in normal cells, it is highly glycosylated and has relatively low affinity for HA in the absence of inflammation (27–29). Therefore, chemotherapeutic conjugation with HA is ideal for selectively targeting cancer cells, including lung cancer cells.

The HA-Pt demonstrated improved pharmacokinetics in rats (30) and canines (31), represented by reduced maximum serum concentration (C_{max}), extended $t_{1/2}$, and increased area under the curve (AUC) (30). It also exhibited superior efficacy in mouse xenografts (17–19) compared to cisplatin (21), and showed efficacy in a Phase I/II canine trial for squamous cell cancers (32).

We hypothesize that intratracheal spray of a low dose of the HA-Pt will reach the cancer tissues in the lung efficiently and release high level of cisplatin on lung cancer sites thereby regressing the lung cancer. The overall dose of cisplatin in the HA-Pt by intratracheal spray is expected to be significantly smaller than a systemic dose, thus causing minimized or reduced side effects.

In the present study, we have developed a lyophilized formulation of the HA-Pt that is freeze-dried immediately after it is synthesized. This formulation is stable, has a long shelf life, and is easy to use after rehydration. Here we show that the lyophilized formulation of the HA-Pt can effectively inhibit the growth of Lewis lung carcinoma (LLC) cells in two-dimensional (2D) and three-dimensional (3D) cell cultures. A bolus intratracheal (IT) administration of aerosolized HA-Pt significantly attenuated the growth of LLC allografts in syngeneic mice without exhibiting any dose-limiting side effects. Therefore, a pulmonary aerosol administration of the lyophilized formulation of the HA-Pt is a realistic local treatment procedure for lung cancer, and the HA-Pt can be used as a powerful and less toxic local chemotherapy for lung cancer treatment.

MATERIALS AND METHODS

Materials

Mouse Lewis lung carcinoma cells (LLC, CRL-1642), H1299 human lung carcinoma cell line (CRL-5803), H358 bronchioalveolar carcinoma cell line (CRL-5807) and A549 human lung carcinoma cell line (CCL-185), were purchased from the American Type Culture Collection. The cells were not specifically characterized for this study. DMEM, RPMI-1640 and Ham's F12 Nutrient Mixture were from Mediatech, Inc., (Manassas Herndon, VA). Fetal bovine serum (FBS) was purchased from Equitech-bio, Inc. (Kerrville, TX). Penicillin-streptomycin and trypsin-EDTA were from Invitrogen (Carlsbad, CA). Other chemicals were analytical grade.

Cell Culture

LLC cells were grown in DMEM supplemented with 10% v/v FBS and 1% v/v penicillin and streptomycin. H1299 and H358 cells were grown in RPMI-1640 supplemented with 10% v/v FBS and 1% v/v penicillin and streptomycin. A549 cells were grown in Ham's F12 Nutrient Mixture supplemented with 10% v/v FBS and 1% v/v penicillin and streptomycin. These cells were incubated at 37°C in a humidified air atmosphere containing 5% CO_2.

Synthesis of HA-Pt

The HA-Pt was synthesized under USP 797 compounding sterile conditions. Typically, 7.5 L of Water for Injection (WFI, VWR, Radnor, PA) was combined with 15 g of cisplatin (Qilu chemical Co., Zibo, China). Subsequently, 30 g of sodium hyaluronate (HA, Lifecore Biomedical, Chaska, MN) was added, and the pH was adjusted to 6.5 using 6 N NaOH. After 4 days, the unreacted cisplatin and unwanted reaction products were removed by tangential flow filtration (Spectrum Laboratories, Rancho Dominguez, CA) with a 10-kDa MWCO PES membrane, followed by concentration to 6 to 8 mg/mL on a cisplatin basis. The concentrated HA-Pt was terminally sterilized by passage through two sterile 0.22 micron filters (Spectrum Laboratories, Rancho Dominguez, CA).

Lyophilization of HA-Pt

The HA-Pt was lyophilized using a VirTis Advantage benchtop freeze dryer (SP Scientific, Warminster, PA). Prior to lyophilizing, 2.5%wt each trehalose or mannitol was added to the HA-Pt as a cyroprotectant. The pH was adjusted to 6.8 ± 0.1 or 7.4 ± 0.1 using 1 N NaOH. One hundred milliliters of the HA-Pt was aliquoted into twenty 5-mL glass vials and was frozen in a -80°C freezer for 4 h. The vials were transferred to the freeze dryer and kept at -40°C for 1.5 h. The condenser point was set at -70°C. The vacuum setpoint was 100 mTorr. The parameters for primary drying were 30 h at -35°C and 10 mTorr. The parameters for secondary drying were 5 h at 2°C and 10 mTorr, followed by another 5 h at 8°C and 10 mTorr. Once the drying was complete, vials containing the lyophilized HA-Pt were stored at -20°C in the dark.

Determination of the HA-Pt by ICP-MS Analysis

The platinum concentration of HA-Pt was determined using an Agilent 7500 inductively coupled plasma mass spectrometer (ICP-MS, Agilent, Santa Clara, CA). A calibration curve containing 1 to 50 ppb platinum standards was generated to determine the platinum concentration in the samples. A 50 ppb bismuth solution was used as an internal standard. A 25 ppb platinum solution was used as a quality control sample. The acceptance limits for R^2 value of the calibration curve and the recovery of the internal standard were 0.995 and 80-120%, respectively.

Determination of the Purity of the HA-Pt in an Aqueous Solution by HPLC

The contents of small molecule platinum species including free cisplatin, mono-aquated cisplatin (Pt-mono-aqua), and di-aquated cisplatin (Pt-di-aqua) were quantified using an HPLC equipped with a UV detector and an Alltech® 250 mm × 4.6 mm M/M RP8/cation column. The mobile phase was sodium phosphate solution (10 mM, pH 3.0). The flow rate was 0.25 mL/min. The column temperature was 25°C. The injection volume was 5 µL. A series of cisplatin solutions were used as calibration standards. Prior to HPLC analysis, the lyophilized HA-Pt (8.6 mg/mL on cisplatin basis) was reconstituted with distilled water and centrifuged using a Centricon centrifugal filter unit (10 kDa MWCO) at 4,000 rpm at 4°C for 10 min. The passed-through fraction was immediately injected into the HPLC. The peaks of cisplatin, Pt-mono-aqua, and Pt-di-aqua were detected by a UV detector at 283 nm. The peak areas were calculated and the concentration of each Pt species was determined using a calibration curve.

Determination of the Glass Transition Temperatures (Tg) of Various HA-Pt's

The glass transition temperatures (Tg's) of frozen HA, trehalose, mannitol, sucrose, freshly prepared HA-Pt with 2.5% trehalose or 2.5% mannitol, and reconstituted lyophilized HA-Pt with 2.5% trehalose were determined using differential scanning calorimetry (DSC-Q100, TA Instruments). The operating program included three steps: ramping from 25°C to -80°C at 10°C/min, equilibrating at -80°C for 5 min, followed by ramping from -80°C to 25°C at 2°C/min. Thirty microliters of sample were sealed in a hermetic aluminum pan with a lid. A DSC refrigerated cooling system (RCS90, TA Instruments) was equipped to the instrument to permit the operating temperature of -80°C. Glass transition temperatures of the frozen samples were determined using the Universal Analysis 2000 software package.

Hyaluronidase Degradation Assay of the HA-Pt

The hyaluronidase (HAdase) specificity of the lyophilized HA-Pt was evaluated by incubating 1.5 mg/mL HA-Pt (concentration on HA basis) and 1.5 mg/mL HA with 5 µg/mL HAdase in sodium phosphate buffer containing 140 mM NaCl, 16 mM NaH_2PO_4, and 7 mM Na_2HPO_4 at pH 6.4 at 37°C for up to 24 h. Aliquots of digested samples were collected at 0, 1, 2, 4, 6, and 24 h and stored at -80°C until analysis. Samples ($n = 3$) were diluted 5 fold using mobile phase at the time of analysis by size exclusion chromatography (SEC). SEC was perfomed with a Shodex OHpak SB-804 HQ column, coupled with a refractive index (RI) detector. The mobile phase was 5 mM ammonium acetate buffer (pH 5.0). The flow rate was 0.8 mL/min. The column temperature was 40°C. The injection volume was 80 µL.

Cell Viability Analysis

A MTT assay was performed to examine the effect of the HA-Pt on the LLC, H1299, H358 and A549 cell proliferation *in vitro*. In brief, 500 LLC, 2,000 H1299, and 3,000 H358 or A549 cells suspended in 100 μL growth medium were seeded in 96-well plates, respectively. The cancer cells were treated with increasing concentrations of cisplatin (0.03-10 μg/mL) or the HA-Pt (0.1-10 μg/mL) in saline at 24 h after culture, respectively. Cell viability at 72 h after treatment was evaluated by the MTT assay as previously described (33).

Inhibitory Effect of the HA-Pt on the Growth of LLC Spheroids in *In Vitro* 3D Culture

In order to evaluate the HA-Pt on the growth of LLC spheroids, a three-dimensional spheroid assay was performed as described previously with slight modifications (34). Briefly, 50 μL of 1.5% agarose dissolved in DMEM supplemented with 10% FBS, 1% v/v penicillin and streptomycin was added to 96-well plates. An agarose layer was made by allowing it to solidify at room temperature for 10 min. Then 125 of LLC cells were seeded with 300 μL of growth medium on the agarose layer (Day 0). Varying concentrations of cisplatin (0.03-3 μg/mL) and the HA-Pt (0.1-10 μg/mL) were added at Days 6, 8 and 10. The 1/3 of medium was replaced with fresh growth medium at Days 4, 8 and 10. The images of spheroids ($n = 5$) were recorded using an inverted microscope IX51 (Olympus America Inc., Center Valley, PA) equipped with the cellSens Dimension software (Olympus America Inc.) at Days 6, 8, 10 and 12. The spheroid growth was evaluated by spheroid volume and compared as fold change to volume at Day 6. For confocal microscopic observation, 125 of LLC cells were seeded into Corning® Spheroid Microplates (Corning Incorporated, Tewksbury, MA). The spheroid was treated with 1 μg/mL of cisplatin or the HA-Pt at Day 4. The spheroids were stained with 100 μg/mL each of acridine orange for live cell staining and ethidium bromide for dead cell staining at Day 6. The images were taken using confocal microscope LSM 710 (Carl Zeiss Inc., Thornwood, NY) equipped with the ZEN 2012 (Carl Zeiss Inc.).

Mouse Studies

All animal experiments were approved by Kansas State University Institutional Animal Care and Use Committee (#3637) and conducted under strict adherence with the approved guidelines. Wild-type female C57BL/6 mice obtained from the Charles River Laboratories International, Inc. were housed in a clean facility and held for 10 days for acclimatization. Each mouse was injected *via* the tail vein with 1.2×10^6 LLC cells suspended in 200 μL of PBS. Seven days after LLC cell injection, mice were treated intratracheally with PBS, the HA-Pt, or cisplatin ($n = 5$-6), using an intratracheal sprayer (Penn-Century Inc.) with the dose diluted to a total volume of 50 μL of HA-Pt (7.5 ($n = 5$) or 15 mg/kg ($n = 6$)), or 50 μL of cisplatin (7.5 mg/kg ($n = 6$)). Two weeks after the treatments, the mice were sacrificed; the lungs were dissected for the macroscopic and histological analysis of tumor multiplicity and size.

Histological Analysis

Dissected lungs were fixed in 10% phosphate buffered formalin, paraffin embed, thin-sectioned at 4 μm and stained with hematoxylin and eosin (H & E) for histological examination. Quantitative evaluation of tumor nodules in the lungs was performed as previously described (35).

TUNEL Assay

TUNEL assay was carried out using the DeadEnd™ colorimetric TUNEL system (Promega, Madison, WI) as previously described (34). The fold change was calculated by dividing the percentage of TUNEL-positive cells in the treated tumors by those in untreated tumors.

Immunohistochemical Analysis for CD44 in LLC Allografts

To analyze the CD44 expression in LLC tumors, sections were deparaffinized and heat-induced epitope unmasking was performed in the citrate buffer followed by incubation with 3% H_2O_2/methanol for 3 min to block endogenous peroxidase activity. Sections were incubated with polyclonal anti-CD44 antibodies (1:200 dilution, for 18 h at 4°C, NBP1-31488, Novas Bioscience, LLC., Littleton, CO). After the incubation with primary antibodies, sections were induced into reaction with a biotin-conjugated anti-rabbit IgG antibody (Vector Laboratories, Burlingame, CA) at a 1:100 dilution for 1 h at 37°C, followed by reaction with the avidin-biotin-peroxidase complex reagent (Vector Laboratories) for 40 min at 37°C. Reactions were developed with 3, 3'-diaminobenzidine tetrahydrochloride (Sigma) and counterstained lightly with Mayer's hematoxylin. The percentage of intensively stained area and positive cell numbers with CD44 antibodies in tumor nodules was assessed by ImageJ software (National Institutes of Health, Bethesda, MD) in two randomly selected fields in the mice ($n = 6$-12).

Statistical Analysis

All data are reported as mean ± standard deviation. All experiments were conducted with multiple sample determinations. Statistical significance was assessed by unpaired *t*-test or one-way ANOVA followed by Tukey-Kramer method. Group

comparisons were deemed significant for 2-tailed P values below 0.05.

RESULTS

Development of Lyophilized HA-Pt

Previously, the HA-Pt (Fig. 1a) was frozen at -20°C and lyophilized at room temperature without any cyroprotectants. The HA-Pt was found to be very difficult to reconstitute the lyophilized drug due to melt-back or collapse of the polymer cake. To improve the solubility of lyophilized drug, three approaches were investigated, including the addition of a cryoprotectant, pH adjustment, and the use of a temperature controlled freeze dryer during primary and secondary drying phases. Two cryoprotectants, mannitol and trehalose, were evaluated. The glass transition temperatures (T_g's) of frozen mannitol and trehalose alone were determined to be -24.66 and -27.05°C, respectively (Figs. 1b and c). The T_g's of the HA-Pt with 2.5%wt mannitol and 2.5%wt trehalose were -29.78 and -18.79°C, respectively. The collapse temperature (T_c) is usually 2-3° higher than the T_g's. When the HA-Pt was lyophilized at room temperature, both samples collapsed. The lyophilized HA-Pt shrank in size and formed transparent films that were difficult to rehydrate after drying. However, HA-Pt with cyroprotectants were lyophilized at a temperature lower than their collapse temperatures and were successfully reconstituted. Thus, the HA-Pt with 2.5%wt trehalose was selected as the lead formulation due to its higher collapse temperature and better rehydration properties. In addition, three pH conditions including pH 5.8, 6.8, and 7.4 were investigated for their rehydration properties. The HA-Pt with 2.5%wt trehalose at pH 7.4 was completely dissolved in water within 10 s and formed a relatively non-viscous solution. In contrast, the HA-Pt with 2.5%wt trehalose at pH 5.8 became soluble after 1 h at 24°C and appeared viscous.

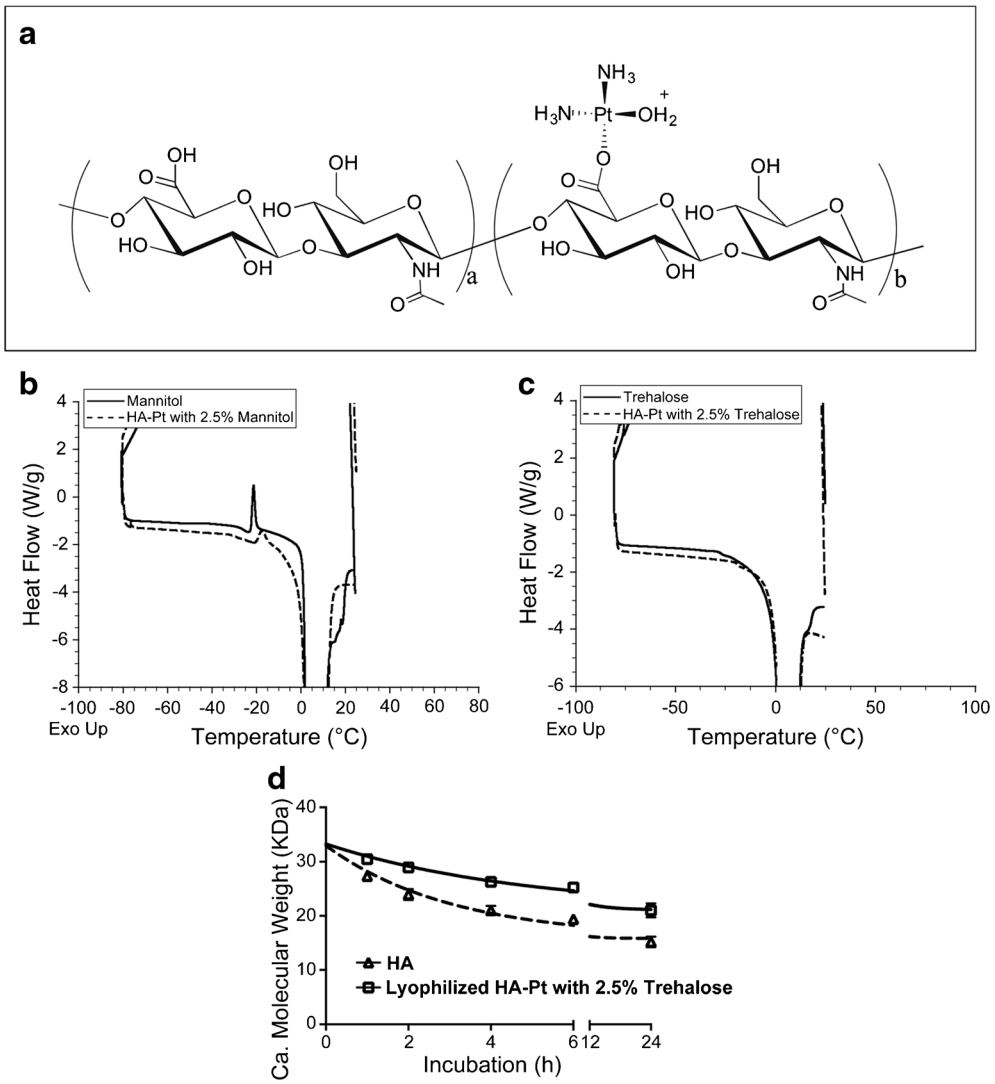

Fig. 1 (**a**) Structure of HylaPlat (HA-Pt), (**b**) Differential scanning calorimetry plots of mannitol and HA-Pt, (**c**) Differential scanning calorimetry plots of trehalose and HA-Pt, and (**d**) Degradation of 35 kDa HA and HA-Pt by hyaluronidase.

Therefore, the HA-Pt with 2.5%wt trehalose and pH 7.4 was selected for further development.

Characterization of the HA-Pt

The concentration of the HA-Pt was determined to be 8.6 mg/mL on a cisplatin basis using ICP-MS. The R^2 value of the platinum calibration curve was 0.998. The quality control samples were within 15% of the nominal values. Each sample was analyzed in triplicates. The cisplatin, Pt-mono-aqua and Pt-di-aqua were isolated from the HA-Pt using a centrifugal filter unit. The retention times of cisplatin, Pt-mono-aqua and Pt-di-aqua were approximately 10.69, 11.35, and 14.05 min. The Pt-mono-aqua and Pt-di-aqua contents were determined to be approximately 0.2 and 0.6%wt using a cisplatin calibration curve ($R^2 = 1$). The hyaluronidase (HAdase) specificity of the lyophilized HA-Pt with 2.5% trehalose was evaluated at 0, 1, 2, 4, 6, and 24 h and compared to unmodified HA. The data was plotted and fitted using GraphPad software. Both the HA and the HA-Pt were successfully degraded by HAdase suggesting that the HA-Pt maintained enzyme specificity and biodegradability (Fig. 1d). The degradation rate constants for the HA and the HA-Pt were 0.3263 and 0.2063 h^{-1}, respectively. The degradation half-lives for the HA and the HA-Pt were 2.125 and 3.360 h. Size exclusion chromatograms were obtained for the formulation that contained HA-Pt and trehalose. The retention times were 11.76 min (HA-Pt) and 13.25 min (trehalose), respectively (Supplemental Figure 1). The sterility, endotoxin, and particulate matter of the HA-Pt was tested by DynaLabs (St. Louis, MO) using the US Pharmacopeia (USP) recommended procedures USP 71, 85, and 788, respectively. The HA-Pt tested negative for aerobic and anaerobic bacteria and fungi (mold and yeasts) during the 14-day sterility testing. The HA-Pt had less than 0.5 EU/mL of endotoxin, which meets the USP limit of $\leq$ 20 EU/mL. The HA-Pt also contained 560 of $\geq$ 10 μm particulates/container, which conformed to the USP limit of $\leq$ 6000, and 443 of $\geq$ 25 μm particulates/container, which met the USP limit of $\leq$ 600. In addition, bioburden testing conducted by Accugen Laboratories (Willowbrook, IL) indicated that the HA-Pt had very low level of spores (<10 cfu per mL), which met and exceeded the generally acceptable limit of 100 cfu per mL.

The HA-Pt Effectively Inhibited Growth of Lung Carcinoma Cells in 2D Cell Culture

The Lewis lung carcinoma cells were treated with increasing concentrations of either cisplatin or the HA-Pt, and the growth rates were compared to untreated controls. At lower platinum concentrations (0.03 or 0.1 μg/mL, Fig. 2a), cell growth was not significantly affected relative to the control. In contrast, it marked anti-proliferative properties of cisplatin and the HA-Pt were shown at higher drug concentrations (Fig. 2a). The cytotoxic profiles and IC_{50} values were similar between cisplatin and the HA-Pt (Fig. 2b). Furthermore, inhibitory effect of HA-Pt on the growth of human lung cancer cell lines was evaluated. As shown in Fig. 3, growths of H1299, H358 and A549 cells were significantly attenuated by HA-Pt in a dose-dependent manner and the effect was similar between cisplatin and the HA-Pt (Fig. 3). The IC_{50} values of the HA-Pt in H1299, H358 and A549 cells were 4.02 μM, 8.39 μM, and 12.42 μM, respectively, while that of cisplatin were 3.44 μM, 5.52 μM, and 8.16 μM, respectively. These results are consistent with the findings of other cell lines in our previous studies (16,17).

The HA-Pt Effectively Induced Cell Death in Tumor Spheroids in 3D Cell Culture

Similar to the result observed in 2D culture, growth inhibition was reported for both cisplatin and the HA-Pt at higher drug concentrations (1 and 3 μg/mL for cisplatin and 1, 3.5 and 10 μg/mL for the HA-Pt). Notably, medium drug concentrations of 0.3 μg/mL for cisplatin or 0.35 μg/mL for the HA-Pt, did not demonstrate the anti-proliferative properties shown in the 2D culture (Fig. 4a). This is likely attributed to the increased physical barriers for drug penetration in the 3D culture model. In contrast to a 2D cell culture model in which drug molecules directly interact with cells and cell surface receptors, a 3D culture model inevitably reduced drug penetration to the interior or the core of the tumor spheroid. As shown in Fig. 4b, however, LLC spheroid growth was inhibited to a greater extent at higher drug concentrations for both cisplatin and the HA-Pt. In the confocal microscopic observation, the tumor spheroids were stained with 100 μg/mL each of acridine orange and ethidium bromide (Fig. 4c) at 48 h after treatment. In the untreated spheroids, live cells stained by acridine orange (green fluorescent) were well packed, and dead cells stained by ethidium bromide (red fluorescent) were mainly detected in the center of spheroids. This pattern is consistent with cell death in the spheroid core due to insufficient oxygen and nutrients. In contrast, dead cells were distributed throughout spheroids in both cisplatin and the HA-Pt-treated spheroids. However, more dead cells were detected in cisplatin-treated spheroids than in the HA-Pt-treated spheroids. Stronger intensity of the green fluorescence in the HA-Pt-treated spheroid suggests that cisplatin possesses a slightly stronger cytotoxicity than that of the HA-Pt. However, it was constantly observed that dead cells (red fluorescent) were more densely localized in the center of the HA-Pt-treated spheroid. This observation may suggest that the HA-Pt possess a high ability to penetrate micro-tumor spheroids.

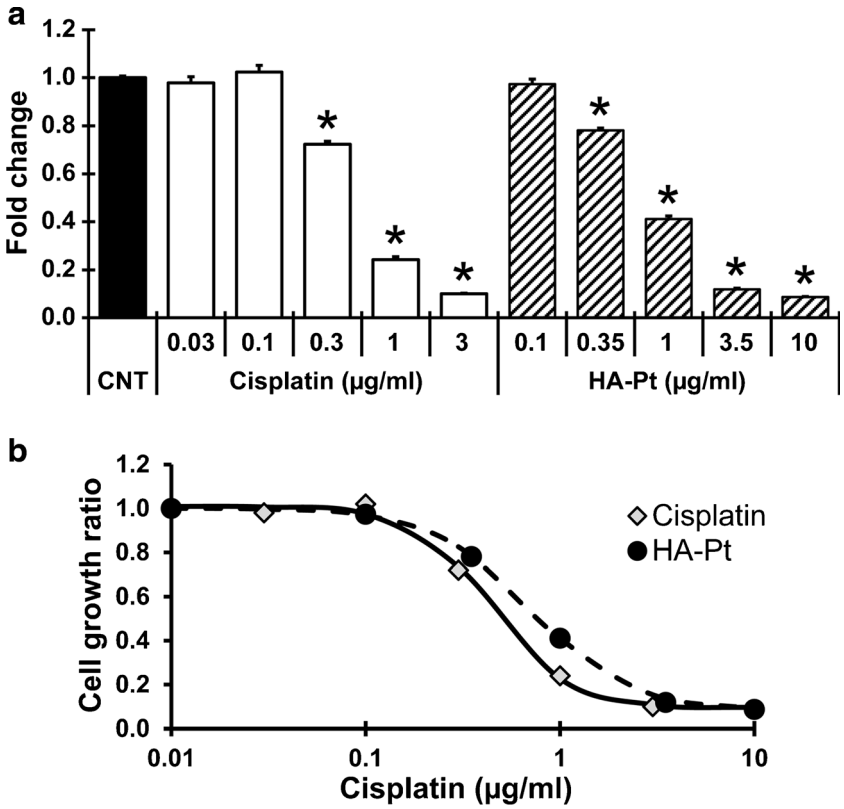

Fig. 2 HA-Pt attenuates LLC cell growth in 2D cell culture. (**a**) Dose-dependent attenuation of LLC cell growth was evaluated by MTT assay. Results are presented as mean ± SD ($n = 3$). *, $p < 0.05$ compared to CNT (Tukey-Kramer method). (**b**) Dose-dependent inhibition curves of LLC cell growth were plotted based on the data in panel A.

The HA-Pt Markedly Inhibited Tumor Growth in Allografts Study in Mice

Administration of the HA-Pt nanoparticles *via* intratracheal spray resulted in significant growth attenuation of lung tumors. Compared to PBS-treated tumor-bearing mice, the HA-Pt-treated mice demonstrated a significantly decreased number of macroscopic tumors (Fig. 5a) as well as reduced sizes of tumor masses (Fig. 5b). Average lung weights (mg) of the 7.5 mg/kg HA-Pt (158.1 ± 34.6) and the 15 mg/kg HA-Pt (215.6 ± 61.7) -treated groups were significantly smaller than that of the PBS-treated group (514.1 ± 109.6, $p < 0.05$) as well as that of the 7.5 mg/kg cisplatin-treated group (349.6 ± 48.1, $p < 0.05$) (Fig. 5b). These results indicate that the tumor growth inhibitory efficacy of the HA-Pt is significantly stronger than unmodified cisplatin at 7.5 mg/kg which is the highest tolerated dose of cisplatin (36). A notable finding of this study is that an even higher dose of the HA-Pt (15 mg/kg), that is above LD_{50} dose of cisplatin, did not cause animal death due to cisplatin acute toxicity, suggesting this HA-Pt formulation of cisplatin is much safer than cisplatin. In addition, histological examination of tumors in H & E stained sections demonstrated a significantly smaller number and size of tumor nodules in mouse lungs treated with the HA-Pt, compared to PBS-treated animals (Fig. 5c and d). Analysis of the HA-Pt-induced apoptosis also suggested that the HA-Pt (7.5 mg/kg) -treated mouse lungs had a statistically significant increase in apoptotic cells compared to PBS-treated mouse lungs (Fig. 5e).

Furthermore, CD44 expression profiles in tumor tissues indicated that the HA-Pt treatment altered the CD44 expression from the cell membrane to cytosolic expression without changing its expression intensity (Fig. 5f and g). On the contrary, the CD44 expression in cisplatin-treated tumors was strong in the plasma membranes and the number of cells with intensive staining was higher than those in PBS or the HA-Pt-treated tumors (Fig. 5f and g). Furthermore, overall CD44 positive cell numbers in the tumor tissues were significantly increased in cisplatin-treated tumors, while it was slightly decreased in HA-Pt-treated tumors compared to those in PBS-treated tumors (Fig. 5h).

DISCUSSION

The primary objectives of this study were to examine the efficacy of pulmonary delivery of the aerosolized HA-Pt as a cisplatin conjugate containing a therapeutic nanoparticle, whether cisplatin can be distributed to the tumor cells throughout the lung and can effectively inhibit lung tumor growth. Results indicated that a single intratracheal spray of the aerosolized HA-Pt caused remarkable tumor growth attenuation without exhibiting noticeable side effects in an orthotopic lung allograft model in syngeneic immunocompetent mice. Furthermore, the efficacy of tumor growth

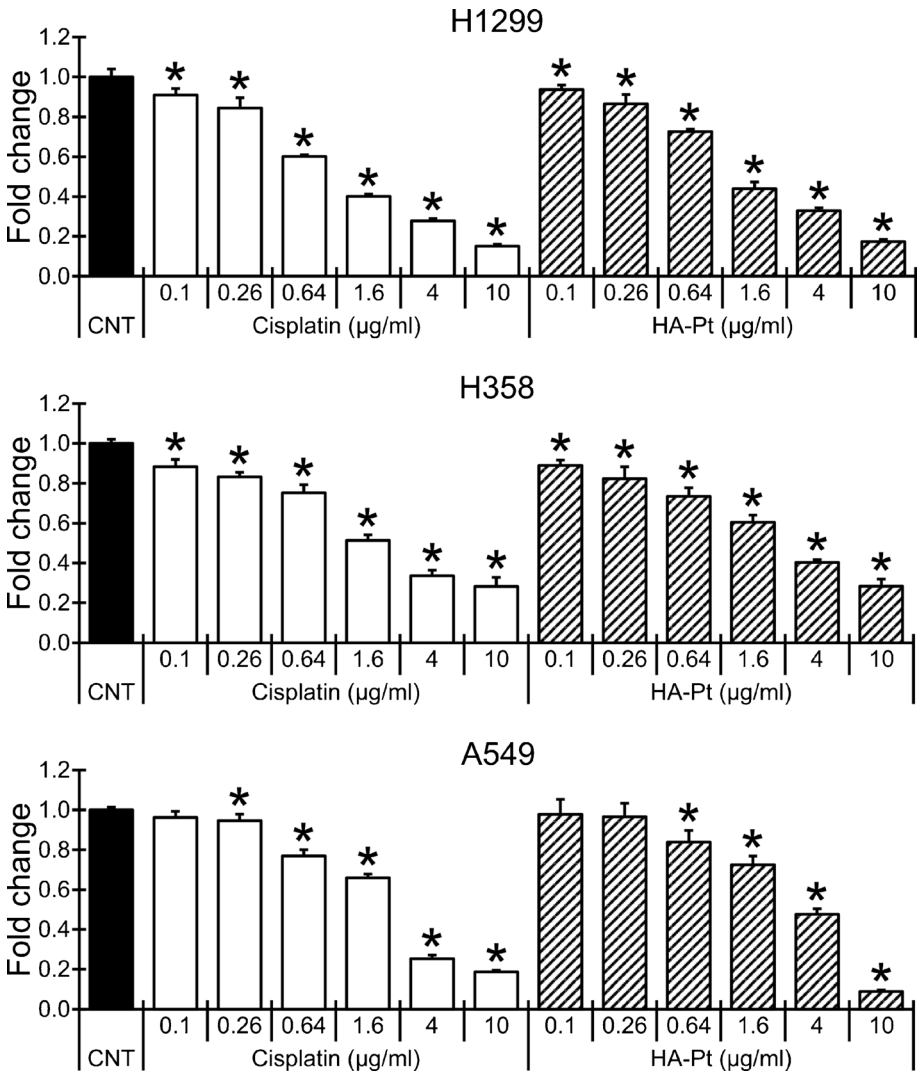

Fig. 3 HA-Pt attenuates growth of human lung cancer cell lines in 2D cell culture. Dose-dependent attenuation of H1299, H358 and A549 cell growth was evaluated by MTT assay. Results are presented as mean ± SD ($n = 3$). *, $p < 0.05$ compared to CNT (Tukey-Kramer method).

attenuation of the HA-Pt is significantly better than the same dose of unmodified cisplatin spray in a parallel study. Therefore, the present study introduces an effective and tolerable *in vivo* cisplatin nanoparticle delivery system for lung cancer therapy.

In the first study, the lyophilized formulation of HA-Pt was developed using trehalose as the cryoprotectant and solubility enhancing agent, examined for its stability and usability in aqueous solution and its biodegradability (Fig. 1). This experiment clearly indicated that newly formulated lyophilized formulation of the HA-Pt is stable with a high solubility in aqueous solution, and hyaluronan is biodegradable by an endogenously available enzyme hyaluronidase, thus its release of cisplatin *in vivo* (Fig. 1d). The HA-Pt was originally developed as a locoregional chemotherapeutic in a liquid form for the treatment of locally advanced cancers that spread *via* the lymphatics, such as breast (16) and lung cancers (37), as well as head and neck squamous cell carcinomas (HNSCC) (17). However, the usability of this liquid formulation of the HA-Pt is limited due to its relatively short shelf life and poor solubility. This newly developed formulation with trehalose was easily solubilized in an aqueous solution, thus higher usability is accomplished. Furthermore, a current animal study (Fig. 5) indicates that this new formulation was applicable to the aerosolized delivery for lung cancer treatment.

In the second study, the therapeutic ability of the HA-Pt was examined in 2D and 3D cell culture studies in comparison with unmodified cisplatin as the control. This study clarified that the HA-Pt is strongly inhibitory to the cell growth of murine lung carcinoma cells in 2D culture and 3D spheroid cell culture (Figs. 2 and 4) and human lung carcinoma cells in 2D culture (Fig. 3). Their IC_{50} values in both 2D and 3D cell cultures revealed that cell growth inhibition by the HA-Pt is as strong as cisplatin. Although it appears that cisplatin-dependent cytotoxicity is slightly stronger than the HA-Pt, the HA-Pt appears to hold high tumor penetration ability, thereby inducing cell death in the deep inside of tumor spheroids (Fig. 4c). This is consistent with the results obtained from the mouse study in which the HA-Pt treatment was significantly more effective in the inhibition of the allograft tumor

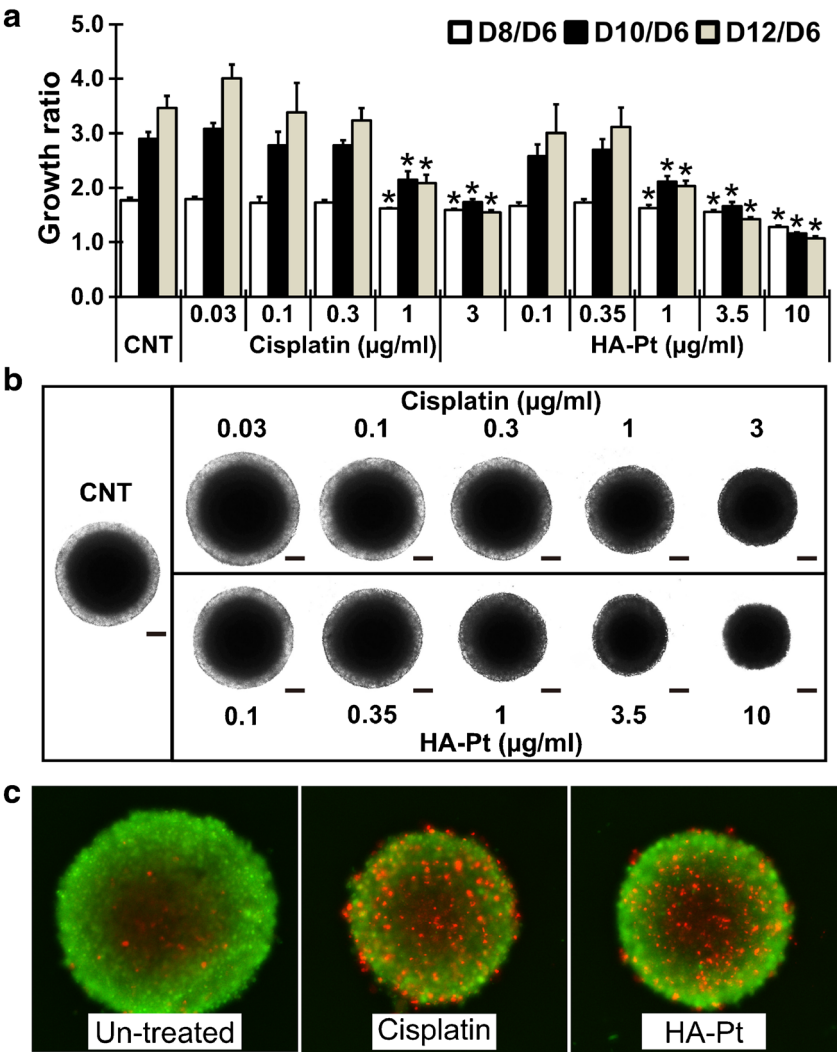

Fig. 4 HA-Pt attenuates LLC growth in 3D spheroid culture. (**a**) Dose-dependent attenuation of LLC spheroid growth. Results are presented as growth ratio of spheroid from Days 6 to 8 (D8/D6), 10 (D10/D6) and 12 (D12/D6). Results are presented as mean ± SD ($n = 5$). *, $p < 0.05$ compared to CNT (Tukey-Kramer method). (**b**) Typical microscopic observation of spheroid growth at Day 12 represented in panel A. (**c**) Images of the untreated, cisplatin, or HA-Pt-treated LLC spheroids. Green fluorescent (acridine orange) indicates live cells. Red fluorescent (ethidium bromide) indicates dead cells. Pictures were taken 2 days after the treatment with 1.0 μg/mL cisplatin or HA-Pt.

growth (Fig. 5). In our previous studies, the HA-Pt liquid formulation demonstrated similar anti-proliferative activity to the parent drug cisplatin in a number of mammalian cancer cell lines *in vitro*, including lung cancer cell line A549; breast cancer cell lines MCF-7, MDA-MB-231, and MDA-MB-468LN; head and neck squamous cell lines MDA-1986 and JMAR; and melanoma cell line A2058 (16,17,19,20,30,37,38). The present study clearly indicated that the cell growth inhibition effect of the new lyophilized formulation of the HA-Pt is similar to the parent cisplatin and the original liquid formulation, suggesting that the newly developed HA-Pt formulation is adequate for the aerosol delivery of this drug as an effective strategy for the treatment of lung cancer.

Having these new data on the lyophilized formulation of the HA-Pt can cause strong growth inhibition of lung cancer cells in 2D and 3D spheroid cell cultures, aerosol delivery of the new HA-Pt was examined using LLC tumor bearing mice. In this experiment, unmodified cisplatin was used as a positive control. As expected, the new HA-Pt treatment attenuated tumor growth macroscopically and microscopically by inducing apoptosis (Fig. 5), indicating that the aerosol delivery of the HA-Pt efficiently distributed the HA-Pt. Quantitative analysis of tumor burdens in each treatment and the degree of apoptosis in the tumors measured by TUNEL assay suggested that a single intratracheal spray of the aerosolized HA-Pt (7.5 mg/kg) induced apoptosis of tumor cells significantly more than the same dose of cisplatin treatment (Fig. 5e), thereby lowering tumor burden more than cisplatin treatment (Fig. 5a, b and d). This mouse study may also suggest that the HA-Pt is a more long-lasting and effective chemotherapeutic than cisplatin. Although the apoptotic index in the higher dose of the HA-Pt treatment group was lower than those in 7.5 mg/kg treated tumors and similar to those in the cisplatin-treated tumors (Fig. 5e), this may be explained by the nonspecific interference of the high dose of the HA-Pt-associated pulmonary edema which was evident in the macroscopic pictures in the Fig. 5a. Although the 15 mg/kg HA-Pt treatment slightly decreased the tumor nodule numbers despite the high dose of the HA-Pt-associated inflammation,

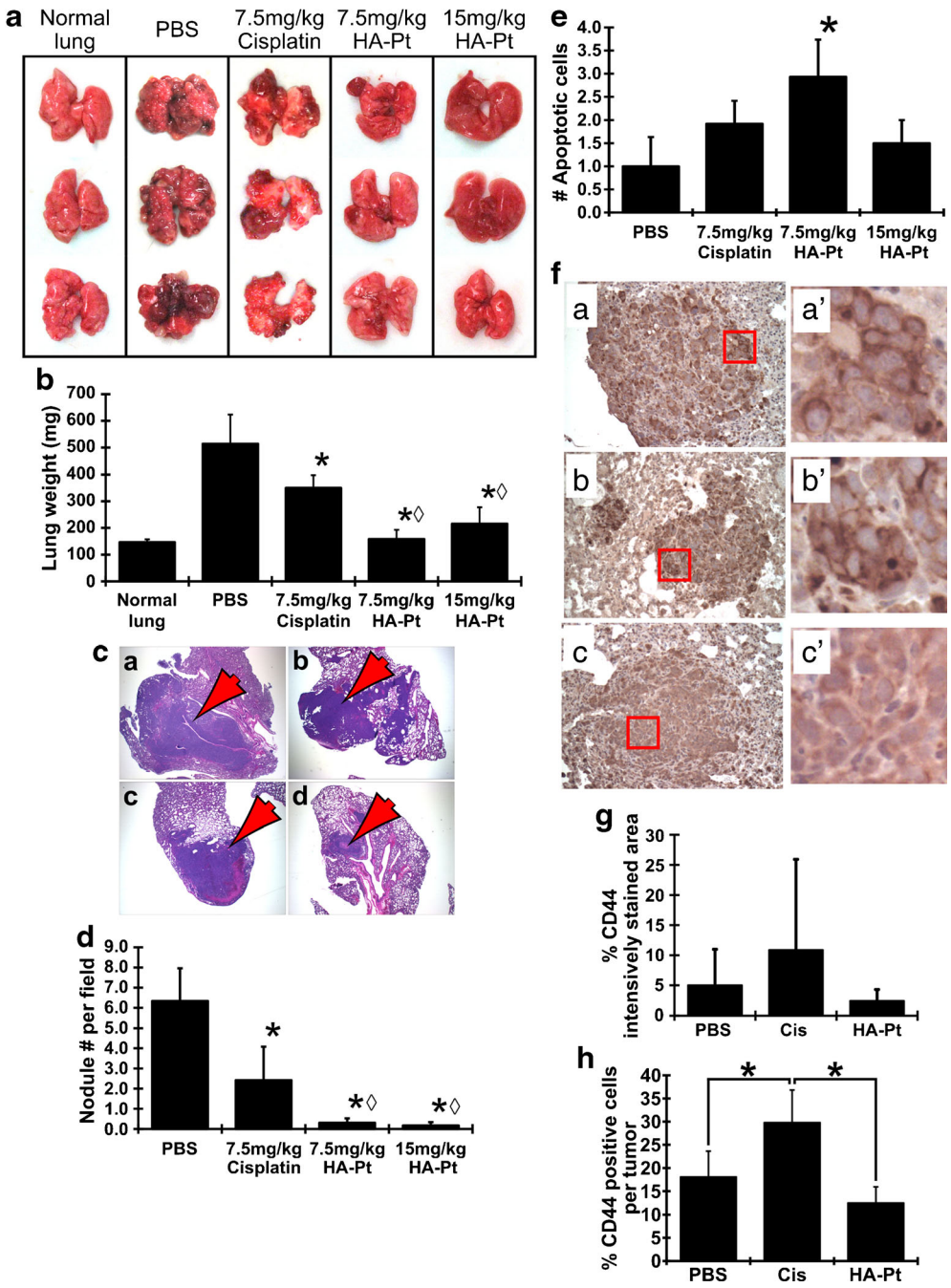

Fig. 5 HA-Pt attenuates growth of LLC tumors in lung. (**a**) Macroscopic view of the lungs in PBS, 7.5 mg/kg cisplatin, 7.5 mg/kg HA-Pt or 15 mg/kg HA-Pt-treated mice. (**b**) Average lung weight in each treatment group were expressed in the bar graphs (n = 5-6). *, $p < 0.05$ as compared with the level of PBS (Welch t-test). ◊, $p < 0.05$ as compared with the level of 7.5 mg/kg cisplatin (Welch t-test). Macroscopic view (**a**) and Average lung weight (**b**) in normal (untreated) mouse is shown as control. (**c**) Typical microscopic views of tumor nodules in the lungs (*arrow*) in PBS (*a*), 7.5 mg/kg cisplatin (*b*), 7.5 mg/kg HA-Pt (*c*), or 15 mg/kg HA-Pt (*d*) -treated mice. (**d**) Average number of tumor nodules in the H & E sections (n = 5-6). *, $p < 0.05$ as compared the level of PBS (Welch t-test). ◊, $p < 0.05$ as compared with the level of 7.5 mg/kg cisplatin (Welch t-test). (**e**) Average number of HA-Pt-induced apoptotic cells in tumor nodules (n = 5-6). *, $p < 0.05$ as compared the level of PBS (Welch t-test). (**f**) Immunohistochemical analysis of the CD44 expression in the tumor nodules in PBS (a and a'), 7.5 mg/kg cisplatin (b and b') and 7.5 mg/kg HA-Pt (c and c') -treated group. Panels a'-c' indicate higher magnification (400× magnification) of red squares in corresponding picture panels a-c (200× magnification). (**g**) Expression intensity of CD44 protein in the lung tumor nodules treated with PBS, 7.5 mg/kg cisplatin or 7.5 mg/kg HA-Pt (n = 6-12). The percentage of intensively stained area with CD44 antibodies were presented. (H) The percentage of CD44 positive cells in the lung tumor nodules treated with PBS, 7.5 mg/kg cisplatin or 7.5 mg/kg HA-Pt (n = 6-12). *, $p < 0.05$ (Welch t-test). All results are presented as mean ± SD.

this 15 mg/kg HA-Pt-dependent decrease of the tumor burden is a small increment. Therefore, this study suggests that the 7.5 mg/kg dose is the adequate therapeutic dose for the aerosol HA-Pt pulmonary administration. Furthermore, the

present study suggests that this dose of the aerosolized HA-Pt pulmonary administration, which is less than a half dosage (28 mg/m^2) of the recommended systemic dosage (60-100 mg/m^2), is tolerable and efficacious in LLC tumor growth inhibition in mouse lungs.

CD44 is a known receptor for HA (23,24) and is highly overexpressed in many cancers, including lung cancer (25,26). It is also known that CD44 is a marker for cancer stem cells (26,39,40) and a potential cause for chemotherapy resistance (41–43). Furthermore, meta-analysis of the patients with lung cancer revealed that CD44 expression was positively correlated with lung cancer progression, advanced metastasis and poor prognosis (25,44). In the 2D cytotoxicity assay of HA-Pt using human lung carcinoma cell lines, A549 cells was less sensitive to the HA-Pt treatment compared to both H1299 and H358 cells (Fig. 3). This may be associated with the CD44 expression levels; lung cancer cells with high CD44 expression may be more sensitive to the HA-Pt treatment. In this regard, it is of interest to cite a few reports that describe the upregulation of CD44 protein in H1299 and H358 cell lines, but not in A549 cell lines (26,45,46).

Immunohistochemical analysis of the CD44 expression in LLC allografts indicated that the HA-Pt treatment altered the CD44 expression from plasma membrane to predominantly cytosol (Fig. 5f); whereas the cisplatin treatment tends to increase the number of cells with intensive staining in the tumors without changing its expression pattern in the tumor cells (Fig. 5f). Since the HA-Pt is shown to be internalized *via* CD44 mediated endocytosis, whereas cisplatin enters into cells *via* diffusion (23), it is likely that the changes of CD44 protein expression in the HA-Pt treated tumors are due to the HA-Pt-induced CD44 translocation. On the contrary, cisplatin diffuses into the cytosol without CD44 mediated mechanism, thus the CD44 protein staining pattern retains the plasma membrane pattern. Furthermore, cisplatin appears to be effective in inducing cell death in CD44 low expressing cancer cell population. This notion is supported by the significant increase of CD44 positive cell numbers in the cisplatin-treated tumors but not in HA-Pt-treated tumors (Fig. 5h). These results may indicate that the HA-Pt treatment is more effective in inducing cell death in CD44 positive and more tumorigenic cell populations among tumor cells. This speculation may explain a better therapeutic efficacy of the HA-Pt treatment than cisplatin (Fig. 5b). In this regard it is noteworthy to cite reports that describe tumorigenic properties (26,39,40) and chemotherapy resistant properties of CD44 positive cancer cells (41–43). Therefore, this observation rationally indicates the superiority of the HA-Pt over cisplatin in lung cancer therapy.

The original formulation of the HA-Pt has demonstrated superior pharmacokinetics and advantageous biodistribution compared to cisplatin *via* locoregional delivery routes such as intratracheal instillation (37), subcutaneous injections (16–20,30,38), and intratumoral injections (21). Since the HA-Pt conjugation in the new lyophilized formulation with trehalose is unchanged, it is conceivable that the new formation of the HA-Pt possesses superior pharmacokinetics than cisplatin. This assumption is supported by the significantly better efficacy in tumor growth inhibition in the present study (Fig. 5) despite similar cell growth inhibition efficacy in 2D and 3D cell culture studies (Figs. 2 and 4). However, the pharmacokinetics of the new formulation of the HA-Pt with pulmonary delivery must be confirmed in the setting of a separate experiment.

Previously, a Phase I study with aerosolized Sustained Release Lipid Inhalation Targeting (SLIT) cisplatin was carried out using 18 patients with lung carcinoma (47). Clinical results suggested that aerosolized SLIT cisplatin was well tolerated, and no dose-limiting toxicity was reported at the maximum delivered dose. The overall response was satisfactory with stable disease in 12 patients and progressive disease in 4 patients. This result is indicative of the safety and feasibility of the inhalation administration of the prolonged-release cisplatin formulation.

The HA-Pt nanoparticles are approximately 25 nm in size (30), which allows it to enter the lymphatic system and migrate to the lung draining lymph nodes *via* the lymphatic vessels (37). Lung cancers are highly metastatic and spread *via* the lymphatic system prior to their systemic dissemination. Our cisplatin delivery system not only offers local disease control, but also controls lymphatic metastases, providing additional benefits compared to other aerosolized formulations of conventional small-molecule chemotherapeutics. Furthermore, the delivery vehicle hyaluronan utilized in the present study is a natural biomolecule produced by all vertebrate animals; thus, it is biodegradable, biocompatible, and absent of undesired toxins. Due to these characteristics, the HA-Pt is a feasible molecule for further development and translational to clinical studies. To the best of our knowledge, this is the first report that describes a successful intratracheal application of the aerosolized form of HA-Pt for lung cancer treatment.

CONCLUSION

We have evaluated the feasibility, safety, and efficacy of a polymeric cisplatin delivery platform, HA-Pt, *via* intratracheal administration using an aerosol spray in mice with lung tumors. The formulation and the route of delivery have shown to be feasible, tolerable, and efficacious against lung cancer. The sustained-release of the HA-Pt nanoparticles successfully suppressed cancer progression and reduced tumor burden. The *in vivo* result was consistent with the *in vitro* findings from both the 2D and the 3D cell culture models. The promising results in rodents may lead to future investigations of the

pharmacokinetics, toxicities, and treatment outcome of the HA-Pt in a larger animal model of naturally occurring lung cancers.

ACKNOWLEDGMENTS AND DISCLOSURES

This work was also supported in part by Kansas State University Johnson Cancer Research Center (MT), Kansas Bioscience Authority Research grant (MLF) and NIH grant 1R01CA173292 (MLF).

We are grateful to Dr. Raelene Wouda (Department of Clinical Science, Kansas State University) for constructive comments during the preparation of the manuscript. We also thank Mr. Joel Sannemann (Department of Anatomy and Physiology, Kansas State University) for his technical support on the confocal microscope.

M.L. Forrest, W.C. Forrest, S. Cai and T. Zhang are employees and/or have ownership interest in HylaPharm, which has licensed HylaPlat technologies from the University of Kansas. No potential conflicts of interest were disclosed by the other authors.

REFERENCES

1. Howlader N, Noone A, Krapcho M, Garshell J, Miller D, Altekruse S, Kosary C, Yu M, Ruhl J, Tatalovich Z, Mariotto A, Lewis D, Chen H, Feuer E, Cronin Ke. SEER Cancer Statistics Review, 1975-2012, National Cancer Institute. Bethesda, MD, http://seer.cancer.gov/csr/1975_2012/, based on November 2014 SEER data submission, posted to the SEER web site, 2015.
2. Siegel RL, Miller KD, Jemal A. Cancer statistics, 2015. CA Cancer J Clin. 2015;65(1):5–29.
3. Blanco E, Hsiao A, Mann AP, Landry MG, Meric-Bernstam F, Ferrari M. Nanomedicine in cancer therapy: innovative trends and prospects. Cancer Sci. 2011;102(7):1247–52.
4. Chow EK, Ho D. Cancer nanomedicine: from drug delivery to imaging. Sci Transl Med. 2013;5(216):216rv214.
5. Ediriwickrema A, Saltzman WM. Nanotherapy for cancer: targeting and multifunctionality in the future of cancer therapies. ACS Biomater Sci Eng. 2015;1(2):64–78.
6. Ryan SM, Brayden DJ. Progress in the delivery of nanoparticle constructs: towards clinical translation. Curr Opin Pharmacol. 2014;18:120–8.
7. Pisters KM, Evans WK, Azzoli CG, Kris MG, Smith CA, Desch CE, *et al.* Cancer Care Ontario and American Society of Clinical Oncology adjuvant chemotherapy and adjuvant radiation therapy for stages I-IIIA resectable non small-cell lung cancer guideline. J Clin Oncol. 2007;25(34):5506–18.
8. Rajeswaran A, Trojan A, Burnand B, Giannelli M. Efficacy and side effects of cisplatin- and carboplatin-based doublet chemotherapeutic regimens versus non-platinum-based doublet chemotherapeutic regimens as first line treatment of metastatic non-small cell lung carcinoma: a systematic review of randomized controlled trials. Lung Cancer. 2008;59(1):1–11.
9. Reed E, Chabner B. Platinum analoges. Phildelphia: Lippincott Williams & Wilkins; 2011.
10. de Castria TB, da Silva EM, Gois AF, Riera R. Cisplatin versus carboplatin in combination with third-generation drugs for advanced non-small cell lung cancer. Cochrane Database Syst Rev. 2013;8, CD009256.
11. Winton T, Livingston R, Johnson D, Rigas J, Johnston M, Butts C, *et al.* Vinorelbine plus cisplatin vs. observation in resected non-small-cell lung cancer. N Engl J Med. 2005;352(25):2589–97.
12. Kelly K, Crowley J, Bunn Jr PA, Presant CA, Grevstad PK, Moinpour CM, *et al.* Randomized phase III trial of paclitaxel plus carboplatin versus vinorelbine plus cisplatin in the treatment of patients with advanced non–small-cell lung cancer: a Southwest Oncology Group trial. J Clin Oncol. 2001;19(13):3210–8.
13. Casagrande N, Celegato M, Borghese C, Mongiat M, Colombatti A, Aldinucci D. Preclinical activity of the liposomal cisplatin lipoplatin in ovarian cancer. Clin Cancer Res. 2014;20(21):5496–506.
14. Stathopoulos GP. Liposomal cisplatin: a new cisplatin formulation. Anticancer Drugs. 2010;21(8):732–6.
15. Go RS, Adjei AA. Review of the comparative pharmacology and clinical activity of cisplatin and carboplatin. J Clin Oncol. 1999;17(1):409–22.
16. Cai S, Xie Y, Bagby TR, Cohen MS, Forrest ML. Intralymphatic chemotherapy using a hyaluronan-cisplatin conjugate. J Surg Res. 2008;147(2):247–52.
17. Cai S, Xie Y, Davies NM, Cohen MS, Forrest ML. Carrier-based intralymphatic cisplatin chemotherapy for the treatment of metastatic squamous cell carcinoma of the head & neck. Ther Deliv. 2010;1(2):237–45.
18. Cohen SM, Rockefeller N, Mukerji R, Durham D, Forrest ML, Cai S, *et al.* Efficacy and toxicity of peritumoral delivery of nanoconjugated cisplatin in an in vivo murine model of head and neck squamous cell carcinoma. JAMA Otolaryngol Head Neck Surg. 2013;139(4):382–7.
19. Cohen MS, Cai S, Xie Y, Forrest ML. A novel intralymphatic nanocarrier delivery system for cisplatin therapy in breast cancer with improved tumor efficacy and lower systemic toxicity in vivo. Am J Surg. 2009;198(6):781–6.
20. Yang Q, Aires DJ, Cai S, Fraga GR, Zhang D, Li CZ, *et al.* In vivo efficacy of nano hyaluronan-conjugated cisplatin for treatment of murine melanoma. J Drugs Dermatol: JDD. 2014;13(3):283–7.
21. Venable R, Worley D, Gustafson D, Hansen R, Ehrhart E, Cai S, *et al.* Hyaluronan cisplatin conjugate in five dogs with soft tissue sarcomas. Am J Vet Res. 2012;73(12):1969–76.
22. Brown TJ. The development of hyaluronan as a drug transporter and excipient for chemotherapeutic drugs. Curr Pharm Biotechnol. 2008;9(4):253–60.
23. Cai S, Alhowyan AA, Yang Q, Forrest WC, Shnayder Y, Forrest ML. Cellular uptake and internalization of hyaluronan-based doxorubicin and cisplatin conjugates. J Drug Target. 2014;22(7):648–57.
24. Maiolino S, Moret F, Conte C, Fraix A, Tirino P, Ungaro F, *et al.* Hyaluronan-decorated polymer nanoparticles targeting the CD44 receptor for the combined photo/chemo-therapy of cancer. Nanoscale. 2015;7(13):5643–53.
25. Ko YH, Won HS, Jeon EK, Hong SH, Roh SY, Hong YS, *et al.* Prognostic significance of CD44s expression in resected non-small cell lung cancer. BMC Cancer. 2011;11:340.
26. Leung EL, Fiscus RR, Tung JW, Tin VP, Cheng LC, Sihoe AD, *et al.* Non-small cell lung cancer cells expressing CD44 are enriched for stem cell-like properties. PLoS One. 2010;5(11), e14062.
27. Orian-Rousseau V. CD44, a therapeutic target for metastasising tumours. Eur J Cancer. 2010;46(7):1271–7.
28. Petrey AC, de la Motte CA. Hyaluronan, a crucial regulator of inflammation. Front Immunol. 2014;5:101.
29. Zoller M. CD44: can a cancer-initiating cell profit from an abundantly expressed molecule? Nat Rev Cancer. 2011;11(4):254–67.
30. Cai S, Xie Y, Davies NM, Cohen MS, Forrest ML. Pharmacokinetics and disposition of a localized lymphatic polymeric hyaluronan conjugate of cisplatin in rodents. J Pharm Sci. 2010;99(6):2664–71.

31. Venable ROWD, Gustafson DL, Hansen RJ, Ehrhart III EJ, Cai S, Cohen MS, *et al.* Effects of intratumoral administration of a hyaluronan-cisplatin nanoconjugate to five dogs with soft tissue sarcomas. Am J Vet Res. 2012;73(12):1969–76.
32. Cai S, Zhang T, Forrest WC, Yang Q, Groer C, Mohr E, Aires DJ, Axiak-Bechtel SM, Flesner BK, Henry CJ, Selting KA, Tate D, Swarz JA, Bryan JN, Forrest ML. Phase I/II Clinical Trial of Hyaluronan-Cisplatin Nanoconjugate for the Treatment of Spontaneous Canine Cancers. American Journal of Veterinary Research. 2015;Accepted.
33. Pickel L, Matsuzuka T, Doi C, Ayuzawa R, Maurya DK, Xie SX, *et al.* Overexpression of angiotensin II type 2 receptor gene induces cell death in lung adenocarcinoma cells. Cancer Biol Ther. 2010;9(4):277–85.
34. Friedrich J, Seidel C, Ebner R, Kunz-Schughart LA. Spheroid-based drug screen: considerations and practical approach. Nat Protoc. 2009;4(3):309–24.
35. Matsuzuka T, Rachakatla RS, Doi C, Maurya DK, Ohta N, Kawabata A, *et al.* Human umbilical cord matrix-derived stem cells expressing interferon-beta gene significantly attenuate bronchioloalveolar carcinoma xenografts in SCID mice. Lung Cancer. 2010;70(1):28–36.
36. Lewis RJ, Sax NI. Sax's dangerous properties of industrial materials. New York: Van Nostrand Reinhold; 1996.
37. Xie Y, Aillon KL, Cai S, Christian JM, Davies NM, Berkland CJ, *et al.* Pulmonary delivery of cisplatin-hyaluronan conjugates via endotracheal instillation for the treatment of lung cancer. Int J Pharm. 2010;392(1-2):156–63.
38. Cohen SM, Mukerji R, Cai S, Damjanov I, Forrest ML, Cohen MS. Subcutaneous delivery of nanoconjugated doxorubicin and cisplatin for locally advanced breast cancer demonstrates improved efficacy and decreased toxicity at lower doses than standard systemic combination therapy in vivo. Am J Surg. 2011;202(6):646–52. discussion 652-643.
39. Al-Hajj M, Wicha MS, Benito-Hernandez A, Morrison SJ, Clarke MF. Prospective identification of tumorigenic breast cancer cells. Proc Natl Acad Sci U S A. 2003;100(7):3983–8.
40. Patrawala L, Calhoun T, Schneider-Broussard R, Li H, Bhatia B, Tang S, *et al.* Highly purified CD44+ prostate cancer cells from xenograft human tumors are enriched in tumorigenic and metastatic progenitor cells. Oncogene. 2006;25(12):1696–708.
41. Liu J, Xiao Z, Wong SK, Tin VP, Ho KY, Wang J, *et al.* Lung cancer tumorigenicity and drug resistance are maintained through ALDH(hi)CD44(hi) tumor initiating cells. Oncotarget. 2013;4(10):1698–711.
42. Torre C, Wang SJ, Xia W, Bourguignon LY. Reduction of hyaluronan-CD44-mediated growth, migration, and cisplatin resistance in head and neck cancer due to inhibition of Rho kinase and PI-3 kinase signaling. Arch Otolaryngol Head Neck Surg. 2010;136(5):493–501.
43. Yoon C, Park do J, Schmidt B, Thomas NJ, Lee HJ, Kim TS, *et al.* CD44 expression denotes a subpopulation of gastric cancer cells in which Hedgehog signaling promotes chemotherapy resistance. Clin Cancer Res. 2014;20(15):3974–88.
44. Luo Z, Wu RR, Lv L, Li P, Zhang LY, Hao QL, *et al.* Prognostic value of CD44 expression in non-small cell lung cancer: a systematic review. Int J Clin Exp Pathol. 2014;7(7):3632–46.
45. Matsubara Y, Katoh S, Taniguchii H, Oka M, Kadota J, Kohno S. Expression of CD44 variants in lung cancer and its relationship to hyaluronan binding. J Int Med Res. 2000;28(2):78–90.
46. Quan YH, Kim B, Park JH, Choi Y, Choi YH, Kim HK. Highly sensitive and selective anticancer effect by conjugated HA-cisplatin in non-small cell lung cancer overexpressed with CD44. Exp Lung Res. 2014;40(10):475–84.
47. Wittgen BP, Kunst PW, van der Born K, van Wijk AW, Perkins W, Pilkiewicz FG, *et al.* Phase I study of aerosolized SLIT cisplatin in the treatment of patients with carcinoma of the lung. Clin Cancer Res. 2007;13(8):2414–21.